

Received March 19, 2021, accepted April 10, 2021, date of publication April 13, 2021, date of current version April 23, 2021.

Digital Object Identifier 10.1109/ACCESS.2021.3073000

Precise Angle Estimation by Jointly Using Spatial/Temporal Change of Channel State Information and Its Application in Pedestrian Positioning

WATARU KOMAMIYA¹, SUHUA TANG¹, (Member, IEEE), AND SADAO OBANA²

¹Department of Computer and Network Engineering, Graduate School of Informatics and Engineering, The University of Electro-Communications, Chofu 182-8585, Japan

²The University of Electro-Communications, Chofu 182-8585, Japan

Corresponding author: Suhua Tang (shtang@uec.ac.jp)

This work was supported by the Japan Society for the Promotion of Science (JSPS) KAKENHI under Grant 19K11937.

ABSTRACT Previously, we have proposed a pedestrian positioning method that uses vehicles near a pedestrian as anchors, and combines vehicle-to-vehicle (V2V) communication signals and GPS signals for high precision positioning. In this method, pedestrian-vehicle distance and angle of arrival (AoA) are estimated from the channel state information (CSI) of vehicular signals and used in position computation, but the precision of angle estimation is limited due to the small number of antennas that can be mounted on a mobile device. To solve this problem, in this paper, we propose a new method to estimate AoA precisely by jointly using spatial change of CSI at multiple antennas and temporal change of CSI per antenna (caused by pedestrian/vehicle movement), and on this basis improve pedestrian positioning precision. Specifically, a two-dimensional antenna array is constructed from CSI acquired from multiple antennas/timings, and the MUSIC method with spatial smoothing is applied to estimate AoA. 3D ray tracing simulations with real 3D map confirm that the proposed method can effectively improve the precision of angle estimation and reduce positioning error when only a small number of antennas are available at a pedestrian device, and the performance increases with the number of antennas.

INDEX TERMS Angle of arrival, virtual antenna array, channel state information, doppler shift, pedestrian positioning, pedestrian-to-vehicle communication.

I. INTRODUCTION

Technologies for preventing traffic accidents, such as vehicle-to-vehicle (V2V) and pedestrian-to-vehicle (P2V) communications, are being actively studied. In V2V communication, vehicles mutually exchange their position and speed information to warn drivers of potential collisions based on the predicted inter-vehicle distance. Actually, V2V, using the 700MHz band, has already been put into practical use in Japan since 2015 [1]–[3]. In P2V communication, a pedestrian's mobile device notifies its position to nearby vehicles to prevent collision accidents [4]. This method enables a vehicle to detect a pedestrian in the blind spot behind a building, which is impossible for other methods that use camera or LiDAR sensor and only work in the line-of-sight

environment. But its reliability heavily depends on the precision of pedestrian position.

In outdoor environments, generally position information is computed by using GNSS (Global Navigation Satellite System) such as GPS (Global Positioning System). In this method, computing the position of a receiver requires at least four satellites (by using satellite positions and satellite-receiver distances acquired from satellite signals). However, in urban canyons, satellite signals are often obstructed and reflected by high buildings, which either make it impossible to compute a position (the number of satellites is not sufficient) or increase the positioning error due to using reflected signals [5]. The number of satellites can be increased by integrating GPS with other satellite systems, e.g., Galileo, GLONASS, Beidou and QZSS (Quasi-Zenith Satellite System) [6], but their performance improvement is still limited in urban canyons because the available satellites are concentrated near the zenith.

The associate editor coordinating the review of this manuscript and approving it for publication was Wei Jiang.

For this reason, a vehicle does not merely rely on GPS to compute its position, but also corrects its position by using other methods such as Dead Reckoning, map matching and lane detection. In this way, the vehicle positioning error can be reduced to sub-meters even in urban canyons [7], [8]. In addition, an autonomous driving car is expected to have much higher positioning precision in the future. In comparison, a pedestrian device can hardly effectively correct its position by other methods due to the constraint of its device size and low accuracy of its sensors, which accordingly degrades the performance of P2V communication in urban canyons.

In order to improve pedestrian positioning precision, we previously proposed methods [9], [10] that use directly visible vehicles as anchors and combine V2V communication signals and GPS signals for pedestrian positioning. In these methods, a pedestrian position is calculated by using pedestrian-vehicle distances estimated from channel state information (CSI) of vehicular signals overheard by a pedestrian device. On this basis, other methods [11], [12] were also proposed, which use pedestrian-vehicle angle information in addition to distance information. In [11], angle of arrival (AoA) is estimated from spatial differences of CSI in multiple receiving antennas, and in [12], angle of departure (AoD) is estimated from temporal differences of CSI at multiple receiving timings in a single antenna. But the precision of angle estimated by these methods is still limited because (i) only a small number of antennas are available at a pedestrian device for the AoA estimation and (ii) only temporal change of CSI within a short interval is available for the AoD estimation.

Angle information plays an important role in positioning. To improve the precision of angle estimation with a small number of antennas, some researchers have suggested the sparsity-based methods [13], using two antenna arrays (with N_1 and N_2 antennas respectively) with coprime setting. But it still requires $N_1 + N_2 - 1$ antennas to approximate $N_1 N_2$ antennas, which has a limited performance when N_1 and N_2 are small.

To solve the aforementioned problem, in this paper, we propose a new method to precisely estimate the angle between a pedestrian and a vehicle by introducing a new dimension. The proposed method jointly exploits spatial change of CSI (N antenna) and temporal change of CSI (M receiving timing) to estimate AoA, and uses it to improve pedestrian positioning precision with a small number of antennas at a pedestrian device. Specifically, this method constructs a two-dimensional virtual antenna array (equivalent to MN antennas), by acquiring CSI from multiple receiving timings of signals at multiple antennas, and estimates AoA from phase differences between CSI items in the virtual antenna array.

The contributions of this paper are two-fold, as follows.

- A new method is proposed for angle estimation by jointly using spatial change of CSI (multiple antennas) and temporal change of CSI (multiple receiving times per antenna). To the best of our knowledge, this is the first time to combine the spatial and temporal changes

of CSI for the AoA estimation. The two kinds of information complement each other, which enables precise estimation of AoA with a small number of antennas that can be mounted on mobile devices.

- The proposed method is extensively evaluated by comparing it with the state-of-the-arts, in various environments using 3D ray tracing simulations, considering the factors such as the number of antennas, the frequency band, the number of vehicles as anchors, and vehicle position error.

This paper uses the following notations. In the distance estimation, L is signal strength and d is signal propagation distance. In the angle estimation, N is the number of antennas and l is the distance between adjacent antennas. \mathbf{X} is the vector of signals received at all antennas, θ_A is angle of arrival, and $\mathbf{a}(\theta_A)$ is a steering vector. When CSI along the temporal axis is used, M is the number of CSI acquisitions, Δt is time interval of CSI acquisition, and θ_D is angle of departure. In the position computation, \mathbf{X} is a state vector, \mathbf{Y} is an observation vector, \mathbf{F} is a state transition matrix, \mathbf{P} is a state covariance matrix, \mathbf{H} is an observation model matrix, \mathbf{K} is a Kalman gain matrix, \mathbf{Q} is a process noise covariance matrix, and \mathbf{R} is an observation noise covariance matrix. As for the operators, \otimes is the Kronecker product. The superscript H is complex transpose, T is transpose, $*$ is complex conjugate, $-$ means predicted value while $+$ means updated value in the Kalman filter. Vectors and matrices are represented in the bold font.

In the rest of this paper, Section II reviews related research, Section III describes the proposed method, and Section IV presents simulation settings and results of simulation evaluation. Finally, Section V concludes this paper and points out future works.

II. RELATED RESEARCH

A. BASE METHODS OF PEDESTRIAN POSITIONING

In order to improve pedestrian positioning precision in urban canyons, previous methods [9], [10] use directly visible vehicles, which are assumed to have precise positions, as anchors for pedestrian positioning. A pedestrian device overhears V2V communication signals which contain vehicle position information sent by nearby vehicles, and calculates its own position by estimating pedestrian-vehicle distance from CSI of received vehicular signals. Later, pedestrian-vehicle angle is also estimated from CSI to further improve positioning precision [11], [12].

B. DISTANCE ESTIMATION

Signal propagation distance between a pedestrian and a vehicle is generally estimated from RSSI (Received Signal Strength Indicator), which represents the overall strength of a received signal. A signal transmitted by a transmitter arrives at a receiver through two different types of paths (Left of Figure 1). One is LoS (Line of Sight) path via which the signal arrives directly without reflection/diffraction, and the other is multipath via which the signal is reflected/diffracted. In order to avoid the impact of reflection/diffraction, the propagation distance should be estimated

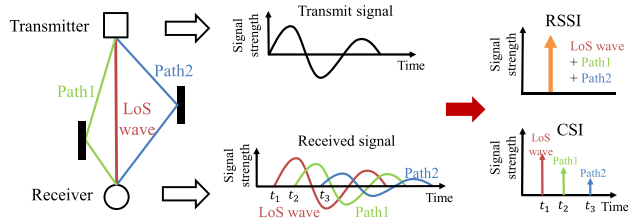


FIGURE 1. Signal propagation paths and the difference between RSSI and CSI.

from the LoS path wave. But RSSI is the sum of all LoS/multipath waves (Upper right of Figure 1), and the distance estimation from RSSI may cause large errors.

In comparison, CSI is acquired from an OFDM (Orthogonal Frequency Division Multiplexing, which is used in Wi-Fi and LTE) modulated signal, and indicates the signal strength/phase of each path in the time/frequency domain (Lower right of Figure 1) [14]. For this reason, the strength of each individual LoS/multipath wave can be acquired from CSI if the time resolution of a receiver is high enough to separate paths, and the precision of distance estimation is improved compared with the case where RSSI is used.

Pedestrian-vehicle distance, as the signal propagation distance of the LoS wave, is estimated based on the relationship between the strength of the LoS path wave (L) and the propagation distance d , as follows:

$$L = a \cdot \log_{10} d + b. \quad (1)$$

Here a and b are constants and can be calculated by a linear regression from pairs of signal strength and propagation distance of the LoS wave.

The propagation distance can also be estimated from the time-of-flight, by exploiting CSI information [15], [16].

C. AOA ESTIMATION IN 2D SPACE

Pedestrian-vehicle angle can be estimated by different methods, leveraging an ESPAR antenna (using simple RSSI information) [17] or an antenna array (using phase information) [11], [18], [19]. When a signal is received by an antenna array, there is a small difference ($\Delta d = l \cdot \cos \theta_A$) in the signal propagation distance between two adjacent antennas (Left of Figure 2), and it causes a signal phase difference $\Delta \varphi = 2\pi \cdot \Delta d / \lambda$, where λ is the wavelength of the signal. Then, the AoA, θ_A , can be derived by using the phase difference of the LoS wave obtained from CSI at each antenna.

Many angle estimation methods have been proposed so far and they can be divided into 3 categories: subspace-based, sparsity-based, and machine learning based methods.

1) SUBSPACE-BASED METHODS

Subspace-based methods include MUSIC (multiple signal classification) [20], ESPRIT [21] and Root-WSF [22]. In the MUSIC method, when K signals (with zero means) arrive at a one-dimensional antenna array with N antennas equally spaced by l , the steering vector representing the phase response to each arrival signal is expressed by $\mathbf{a}(\theta_{A,k})$, where

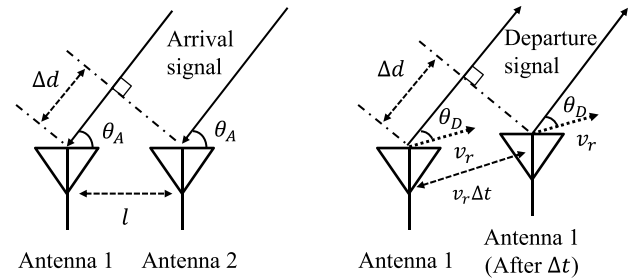


FIGURE 2. Different methods for pedestrian-vehicle angle estimation. Using spatial phase difference at multiple receiving antennas (Left). Using temporal phase difference at multiple receiving timings (Right).

$\theta_{A,k}$ is the AoA of the k th signal. Further assuming that the overall received signal of the n th antenna is \mathbf{x}_n , a vector representing the signals received at all antennas is defined as $\mathbf{X}(t)$ and its covariance matrix is defined as \mathbf{R}_{xx} . Denote the eigenvalues and eigenvectors of \mathbf{R}_{xx} as λ_i and \mathbf{e}_i , respectively, in the descending order of λ_i ($i = 1, 2, \dots, N$). Of these N eigenvectors, K eigenvectors with large eigenvalues correspond to the signal subspace, and the rest correspond to the noise subspace. Using the noise-eigenvectors, the MUSIC spectrum $S(\theta_A)$ is calculated as

$$S(\theta_A) = \frac{1}{\sum_{i=K+1}^N |\mathbf{a}^H(\theta_A) \mathbf{e}_i|^2}. \quad (2)$$

Then, θ_A is estimated from the peak of $S(\theta_A)$.

In this method, the larger the number of receiving antennas, the higher the spatial resolution and the more precise angle estimation becomes. Currently, many mobile devices are equipped with 2-4 antennas [23], and it is difficult to mount a large number of antennas on current mobile devices due to the size limitation.

a: SPATIAL SMOOTHING

In order to apply the MUSIC method to coherent signals such as a LoS wave and its multipath replica sent from the same transmitter, a spatial smoothing method [24] was proposed as a preprocessing step. A one-dimensional antenna array with N antennas is divided into P subarrays, each of which has N_s antennas ($P > N_s$, $P = N - N_s + 1$). Here, subarrays may share common antennas. Then, a vector representing the signals received at all antennas of the p th subarray is defined as

$$\mathbf{X}_p(t) = [\mathbf{x}_p(t), \mathbf{x}_{p+1}(t), \dots, \mathbf{x}_{p+N_s-1}(t)]^T, \quad p = 1, 2, \dots, P \quad (3)$$

and its covariance matrix is computed as \mathbf{R}_p . Then, the average of all \mathbf{R}_p is computed as

$$\mathbf{R}_{SSP} = \frac{1}{P} \sum_{p=1}^P \mathbf{R}_p. \quad (4)$$

If P is no less than D , the number of coherently received signals, the MUSIC method can be applied.

A modified spatial smoothing method [25] was also proposed. In this method, \mathbf{R}_{MSSP} is defined by

$$\mathbf{R}_{MSSP} = \frac{1}{2P} \sum_{p=1}^P \left\{ \mathbf{R}_p + \mathbf{J} \mathbf{R}_p^* \mathbf{J} \right\}, \quad (5)$$

and used instead of \mathbf{R}_{SSP} , where \mathbf{J} is an anti-diagonal identity matrix. The modified spatial smoothing method has a higher correlation suppression effect than the original one, and if $P \geq D/2$, the MUSIC method can be applied.

Since it is necessary to create subarrays in these methods, it is difficult to use spatial smoothing with a small number of antennas, which is the typical case for a pedestrian device. In addition, even if it can be applied, the number of available antennas in each subarray for angle estimation decreases, and the angle precision may even get lower compared with the case where all antennas are used simultaneously.

b: APPLICATION TO 2-D VIRTUAL ANTENNA ARRAY

Normally, the MUSIC method is applied to a one-dimensional antenna array along the spatial axis. Recently, a method was proposed in [26] that virtually constructs a two-dimensional antenna array by jointly using frequency domain of received signal with the spatial antenna array. Then, the MUSIC method is applied to the two-dimensional antenna array by separately defining steering vectors that represent the phase responses for the spatial and frequency axes and combining them together. It virtually increases the number of antennas, but the phase change of the frequency axis is used for estimating the propagation distance of the signal, not for estimating the AoA. Therefore, its improvement of angle estimation precision is limited.

2) SPARSITY-BASED METHODS

To improve the spatial resolution with a limited number of antennas, sparsity-based methods were proposed [13], which exploit a sparse antenna array under the coarray equivalence. Two uniform linear subarrays are used, one has N_1 antennas with an inter-antenna space being N_2 units and the other has N_2 antennas with an inter-antenna space being N_1 units. By choosing N_1 and N_2 to be coprime, this method can resolve about $N_1 N_2$ signals with $N_1 + N_2 - 1$ antennas [27], [28], which is useful for separating the LoS signal from the reflected ones in a reflection-rich environment. But it can hardly be applied to a mobile device that can only support about 2-4 antennas.

3) DEEP LEARNING-BASED METHODS

With the emergence of massive MIMO techniques, the spatial resolution of AoA can be further improved. But both the channel estimation and the angle computation become very complex, not to mention the calibration of the non-perfect antennas. To solve these problems, deep learning is exploited in the AoA estimation [29], [30], and has achieved promising results. But the training stage of a deep model still requires a traditional method (subspace-based or sparsity-based) to provide ground-truth.

4) ANGLE ESTIMATION VIA CSI FROM MULTIPLE RECEIVING TIMINGS

Different from the previous methods that exploit multiple antennas, AoD is estimated using CSI acquired at different timings by utilizing the fact that vehicles move while transmitting the V2V communication signals [12]. When acquiring multiple CSI from multiple packets, accurate time synchronization between the transmitter and the receiver is required. In order to avoid this problem, a pedestrian device acquires CSI at multiple timings in the same packet with a time interval Δt . This leads to a small difference in signal propagation distance $\Delta d = v_r \cdot \Delta t \cdot \cos \theta_D$ based on the pedestrian-vehicle relative speed v_r , Δt and AoD θ_D (Right of Figure 2), and Δd causes signal phase difference $\Delta \varphi = 2\pi \cdot \Delta d / \lambda$. Δd is calculated from the phase difference of the LoS wave acquired from the CSI at each receiving timing, and then it is used for calculating θ_D .

In this method, the angle can be estimated regardless of the number of receiving antennas, but the resolution of the estimation is limited because the phase difference of CSI acquired in the same packet is smaller than that acquired by an antenna array and it cannot benefit from multiple antennas. Therefore, its precision is inferior to that in [11] if the number of antennas is increased.

D. AOA ESTIMATION IN 3D SPACE

Recently, with the emergence of drones, 3D AoA estimation starts to attract research interest. With an antenna array at a ground receiver, the azimuth angle of departure (AAoD), elevation angle of departure (EAoD), azimuth angle of arrival (AAoA), and elevation angle of arrival (EAoA) of a drone (transmitter) is estimated in real-time, mobile environment, using initial estimation of these parameters before the transmitter and receiver start moving [31]. By EMVA (Electromagnetic vector-sensor array), full polarization information of each electromagnetic signal is exploited for more accurate estimation of 3D AoA [32].

E. A SHORT COMPARISON

CSI from multiple antennas (spatial) [11] and from multiple receiving timings (temporal) [12] can be acquired simultaneously, but were not used together in previous work because the two methods use different theories for the angle estimation. In this paper, we investigate how to combine the two to compute more accurate 2D angle information, especially when the number of antennas is small. As for the spatial information, although we focus on the MUSIC method [20], the proposed method can be extended to work with the sparsity-based method [27], [28], used to train a deep model to estimate angle more efficiently, and further extended for 3D angle estimation.

III. PROPOSED METHOD

The proposed method exploits directly visible vehicles, together with GPS satellites, as anchors, and uses both pedestrian-vehicle distance and angle information for pedestrian positioning.

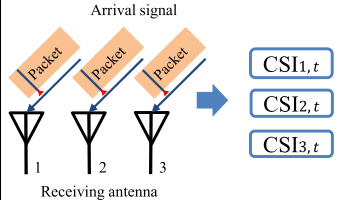
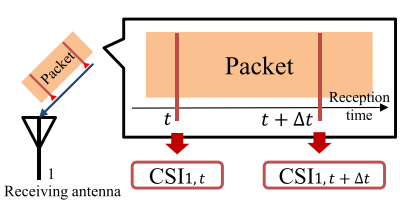
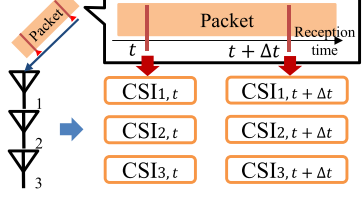
	Base method [11] (S-CSI)	Base method [12] (T-CSI)	Proposed method (J-CSI)
Angle estimation	From phase difference due to <i>spatial difference</i> of CSI	From phase difference due to <i>temporal difference</i> of CSI	From phase difference due to <i>spatial/temporal difference</i> of CSI
Cause of phase difference	Path length difference for each antenna	Channel change due to vehicle movement	Multiple antennas, vehicle movement
Acquisition of multiple CSI	From a received signal of multiple antennas 	From multiple points at a single packet 	From multiple points at a signal of multiple antennas 

FIGURE 3. Comparison between the base methods [11], [12] and the proposed method.

A. OVERVIEW

In order to solve the problem of the base methods [11], [12] that the angle estimation precision is limited with a small number of antennas, we propose a new method to improve the angle precision, constructing a virtual two-dimensional antenna array with spatial/temporal axes by jointly using CSI acquired from multiple antennas/receiving timings, and apply it to improve pedestrian positioning precision. Figure 3 shows a comparison between the base methods [11], [12] and the proposed method. Hereafter, for simplicity, the base methods and the proposed method are referred to as S(Spatial)-CSI [11], T(Temporal)-CSI [12], and J(Joint)-CSI, respectively.

B. PREREQUISITES

Since vehicles usually have high-precision sensors (compared with pedestrians), it is assumed that each vehicle has accurate information on its own position and speed, and broadcasts the information periodically (every 100ms) based on the V2V communication [1]. In addition, it is assumed that pedestrians have mobile devices that can overhear vehicular signals, detect whether vehicles are in line of sight (directly visible) [10], and perform position calculations.

C. ESTIMATION OF PEDESTRIAN-VEHICLE ANGLE

1) CSI ACQUISITION

A pedestrian device overhears a signal transmitted from a surrounding vehicle by a mobile device with N antennas, and each antenna acquires the CSI at M timings, spaced with an interval Δt (e.g. $40\mu s$) in the same packet. Then, a virtual two-dimensional antenna array is constructed from these CSI, as shown in Figure 4.

2) ANGLE ESTIMATION BY THE MUSIC METHOD

The MUSIC method is applied to the two-dimensional antenna array on the spatial/temporal axes to estimate the pedestrian-vehicle angle. In order to enable the application of the MUSIC method to coherent signals, the $N \times M$ virtual antenna array is divided into $(N - N_s + 1) \times (M - M_s + 1)$

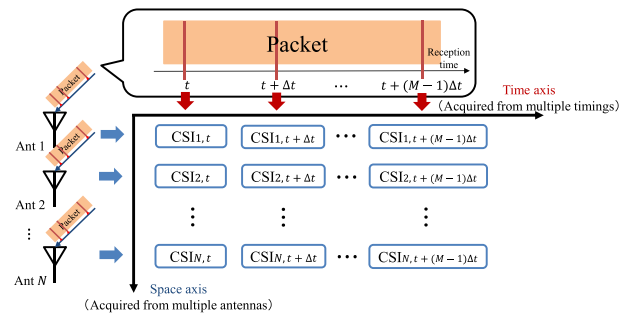


FIGURE 4. Construction of a virtual two-dimensional antenna array.

subarrays each with $N_s \times M_s$ ($N_s < N$, $M_s < M$) virtual antennas, and the modified spatial smoothing method [25] is applied.

Denote $\mathbf{x}_{n,m}$ as the CSI received at the n th antenna and the m th timing, and define $\mathbf{X}_{n,m}(t)$ as a vector representing the CSI of all antennas in a subarray (n th in the spatial axis and m th in the temporal axis), and $\mathbf{R}_{n,m}$ as its covariance matrix, as follows.

$$\mathbf{X}_{n,m}(t) = [\mathbf{x}_{n,m}(t), \mathbf{x}_{n+1,m}(t), \dots, \mathbf{x}_{n+N_s-1,m}(t), \dots, \mathbf{x}_{n,m+1}(t), \dots, \mathbf{x}_{n+N_s-1,m+M_s-1}(t)]^T \quad (6)$$

$$\mathbf{R}_{n,m} = \frac{1}{N_s \times M_s} \mathbf{X}_{n,m}(t) \mathbf{X}_{n,m}^H(t) \quad (7)$$

Then, \mathbf{R}_{MSSP} is calculated as

$$\mathbf{R}_{MSSP} = \frac{1}{2 \times (N - N_s + 1) \times (M - M_s + 1)} \sum_{n=1}^{N-N_s+1} \sum_{m=1}^{M-M_s+1} \{\mathbf{R}_{n,m} + \mathbf{J} \mathbf{R}_{n,m}^* \mathbf{J}\} \quad (8)$$

Let the eigenvalues and eigenvectors of \mathbf{R}_{MSSP} be λ_i and \mathbf{e}_i ($i = 1, 2, \dots, N_s \times M_s$), respectively, in the descending order of λ_i . Of the $N_s \times M_s$ eigenvectors, the first K eigenvectors correspond to the signal subspace, and the remaining

E. COMPARISON WITH OTHER METHODS

When estimating the angle with a mobile device, the limitation of the number of mounted antennas becomes an issue. Subspace based methods such as MUSIC enable precise angle estimation by using a large number of antennas, but have performance degradation when only a small number of antennas (e.g. 2 antennas) are available. Similarly, even with the deep learning-based methods, it is considered difficult to estimate precise angle from limited signal information. High spatial resolution can be obtained from a small number of antennas with sparsity-based methods, but it is difficult to apply to mobile devices which usually can only afford 2-4 antennas.

On the other hand, in J-CSI, the CSI in the temporal axis is jointly used with the CSI of multiple antennas to construct a two-dimensional virtual antenna array, which compensates for the lack of spatial information when the number of antennas is small. Similar to J-CSI, the method [26] uses the CSI in the frequency axis together with the CSI of multiple antennas to construct a two-dimensional virtual antenna array, but only the CSI change among multiple antennas is used for the AoA estimation. In comparison, J-CSI is different in that it uses CSI in both the spatial/temporal axes for the AoA estimation by using the relationship between AoA/AoD of the LoS wave (described in (12)). These features do not exist in other literature.

Similar to the sparsity-based method in some degree, the combination of N antennas (spatial CSI) and M receiving timings (temporal CSI) in J-CSI constructs a virtual antenna array equivalent to MN antennas, which improves the spatial resolution of angle estimation and helps to separate reflected signals from the LoS wave. But it only uses N antennas, instead of $M + N - 1$ in sparsity-based methods. It is also possible to extend the J-CSI method to use spatial CSI by sparsity-based methods.

IV. SIMULATION EVALUATION

The performance of J-CSI is evaluated by comparing it with S-CSI [11], T-CSI [12], ESPRIT [21] and Root-WSF [22] using 3D ray tracing simulation.

A. SIMULATION CONDITIONS

1) SIMULATOR

In the simulation, the software “RapLab”¹ is used to simulate the radio wave propagation from satellites/vehicles to a pedestrian by 3D ray tracing, and the numerical analysis software “MATLAB”² is used to calculate the pedestrian-vehicle distance/angle and the pedestrian position.

2) PLACEMENT OF VEHICLES, PEDESTRIANS AND SATELLITES ON 3D BUILDING MAP

Assuming an urban environment, 3D building map³ around Ginza, Tokyo is used. In order to evaluate the movement of vehicles and a pedestrian, 200 continuous scenes at 100ms

intervals are created, and satellites, vehicles, and pedestrians are placed in each scene. The placement of satellites is based on the actual positions of GPS satellites. Figure 5 shows the trajectories of moving vehicles and a pedestrian on the 3D building map and an aerial photograph of the same area. Only one pedestrian is placed, moving at a speed of 4km/h on the sidewalk. Vehicles are randomly placed on a road with two lanes on each side at intervals of 5-30m and move at a speed of 60km/h. On average there are 10 vehicles in each scene.

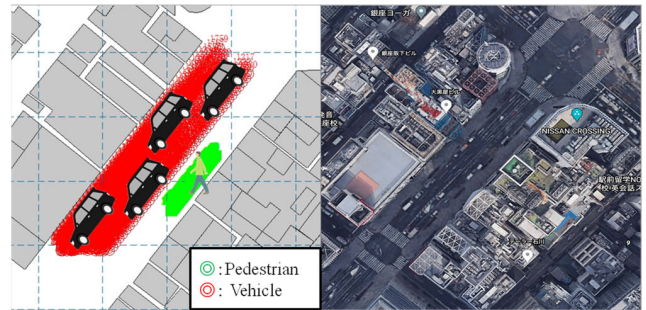


FIGURE 5. Simulation map. Placement of moving vehicles and a pedestrian on the 3D building map (Left). Aerial photograph of the same area (obtained from Google Earth) (Right).

Radio wave propagation information such as CSI is acquired by 3D ray tracing after the placement of satellites, vehicles and a pedestrian. The maximum number of radio wave reflections/diffractions on the terrain or the buildings is set to 1. Based on the V2V communication standard [1], the maximum transmission power is set to 20dBm, the transmission signal frequency is set to 700MHz unless specified otherwise, and vehicular communication is performed at 100ms intervals.

3) SIMULATION OF TIME RESOLUTION

An actual receiver has a limited time resolution. The LoS wave and the subsequent multipath waves that arrive with a time difference less than the time resolution cannot be separated even when CSI is used. In this case, the LoS wave overlaps with some multipath waves, and an error occurs in estimated pedestrian-vehicle distance/angle.

RapLab does not consider this limitation, and CSI can be obtained with all multipath waves separated. In order to perform a simulation close to the real environment, as shown in Figure 6, all waves arriving in the same time resolution (50ns for an off-the-shelf wireless LAN card using 20MHz bandwidth) are combined together. The composite strength of n signals that arrive within the same time resolution is calculated by the following equation.

$$(\gamma_1 + \gamma_2 + \dots + \gamma_n) + i(\delta_1 + \delta_2 + \dots + \delta_n). \quad (23)$$

4) SIMULATION OF THERMAL NOISE

Since noise in the propagation channel is not simulated in RapLab, the influence of thermal noise is added to the CSI by simulating the communication channel. First, using the signal waveform created from random data and the CSI obtained

¹ <https://network.kke.co.jp/products/raplab/>

² <https://www.mathworks.com/>

³ <https://www.aw3d.jp/en/>

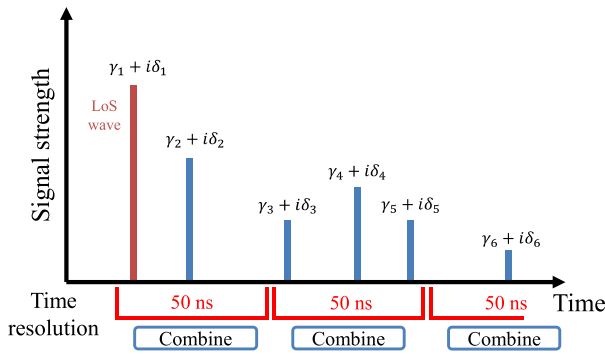


FIGURE 6. Simulation of time resolution of an actual receiver.

in Sec.IV.A.3), the convolution of the OFDM signal and the simulated channel is computed, to which noise is added according to the SNR (Signal to Noise Ratio). Then, from this noisy signal, the CSI is estimated again. Here, the thermal noise power P_n is computed by the following equation.

$$P_n = \frac{hf_c B}{e^{\frac{hf_c}{k_B T}} - 1} \approx k_B T B (hf_c \ll kT) \cdot f_c \quad (24)$$

f_c and B are the center frequency and bandwidth of the signal, respectively, T is the temperature, h is Planck's constant, and k_B is the Boltzmann constant. Assuming a larger noise, $\alpha k_B T B$ (α is a constant) is used as the noise power. In the simulation, $\alpha = 10$, the temperature is 25°C, and the bandwidth is 20MHz.

5) CSI ACQUISITION SETTINGS

Currently, many mobile devices are equipped with 2-4 antennas [23]. Therefore, the number of antennas used to acquire CSI in the spatial axis is assumed to be 2-6 for J-CSI, S-CSI and Root-WSF, 3-6 for ESPRIT, and 1 for T-CSI. Because J-CSI, S-CSI, and Root-WSF use multiple antennas for angle estimation, at least two antennas are required. ESPRIT requires at least three antennas because it divides an antenna array into two sub-arrays for angle estimation. Because T-CSI does not use multiple antennas, the estimation is performed with a single antenna. The number of CSIs acquired in the temporal axis is 6 (at an interval of 40μs) in J-CSI and T-CSI unless specified otherwise, and 1 in S-CSI, ESPRIT and Root-WSF.

6) PEDESTRIAN POSITION CALCULATION

Using the obtained CSI, MATLAB is used to estimate the pedestrian-vehicle distances/angles in each scene and calculate the pedestrian position. The pedestrian-vehicle distance is obtained by inputting the signal strength of the LoS wave into a linear regression model defined by (1). Satellites with an elevation angle of 15 degrees or less are considered to have a large ranging error, and are not used for positioning.

B. RESULTS OF ANGLE ESTIMATION

1) COMPARISON WITH OTHER METHODS

Figure 7 shows how the average angle error changes with the number of antennas in J-CSI, S-CSI, T-CSI, ESPRIT and

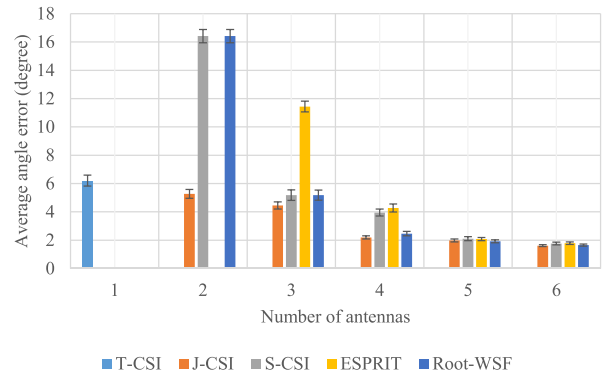


FIGURE 7. Average angle error and 95% confidence interval for each method under different numbers of antennas.

Root-WSF. The results for each method are not shown when the number of antennas is not applicable. In all methods using spatial information, the estimation precision improves with the number of antennas. When the number of antennas is 2, J-CSI reduces the angle error by 68% compared with S-CSI, by 15% compared with T-CSI (with a single antenna). When the number of antennas increases to 6, the performance gain of J-CSI against S-CSI decreases to 9% (and a similar performance gain against ESPRIT and Root-WSF), but increases to 74% when compared with T-CSI.

These results confirm that J-CSI can achieve a particularly large improvement against S-CSI (ESPRIT and Root-WSF) when the number of antennas is small. This is because the low spatial resolution at a small number of antennas is effectively compensated by using CSI acquired at multiple timings in J-CSI. But the difference between J-CSI and S-CSI (ESPRIT and Root-WSF) decreases when more antennas are available, because sufficient angle resolution can be achieved by only using the CSI from multiple antennas.

The precision of J-CSI with two or more antennas is higher than that of T-CSI using a single-antenna, which confirms that the angle resolution, insufficient when only using CSI from multiple timings, is compensated by using the CSI from multiple antennas.

2) COMPARISON OF MUSIC SPECTRUM

Figure 8 shows the true AoA of LoS wave and the MUSIC spectrum of S-CSI and J-CSI calculated for the same signal when 4 antennas are used.

Multipath signal cannot be separated in S-CSI due to insufficient spatial resolution, and a large error occurs in the AoA estimation. In comparison, in J-CSI, the spatial resolution is improved by using the temporal CSI, and the multipath signal (peak near 160 degrees) is separated from the LoS wave, so the error in AoA estimation is small.

3) INFLUENCE OF TRANSMISSION FREQUENCY

The transmission frequency of vehicular signals is changed from 700MHz to 2.4GHz and 5.9GHz that are used in general wireless LAN and VANETs, and the angle estimation error in J-CSI is investigated. The results are shown in Figure 9.

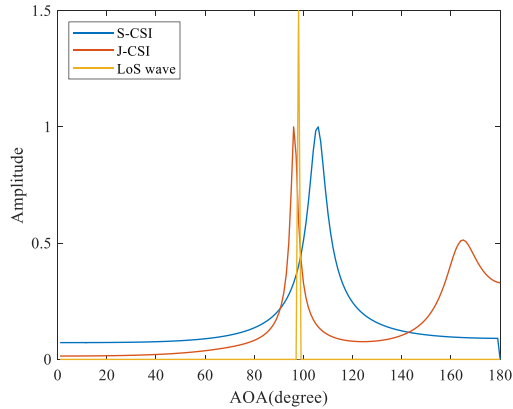


FIGURE 8. True AoA of the LoS wave and the MUSIC spectrum of S-CSI and J-CSI with 4 antennas.

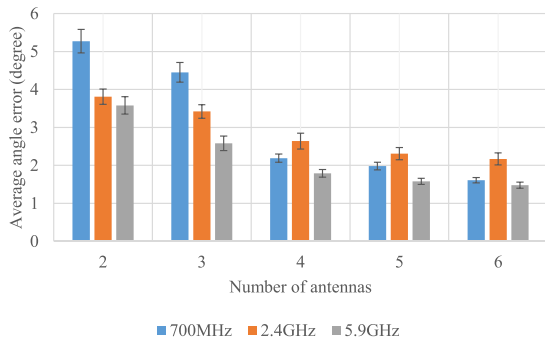


FIGURE 9. Average angle error and 95% confidence interval for each frequency band under different numbers of antennas.

Although the difference in angle error for each frequency is small, the angle error is the lowest at 5.9GHz, and gets larger in the other two frequencies. This is because the signal wavelength λ is in the denominator of the phase difference in (9) and (10), which makes the phase response of each element increase with the frequency. The performance in 2.4GHz is worse than that in 700MHz when 4 or more antennas are used, indicating that increasing the frequency does not always reduce the angle error. This is because the attenuation of the signal increases with the frequency, and the signal strength decreases at 2.4GHz compared to 700MHz, which leads to a lower SNR and an increase in the angle error. This degrades the performance gain brought by the increase of phase response in some degree, and makes the influence of frequency band not so large in the angle estimation.

4) INFLUENCE OF PEDESTRIAN-VEHICLE DISTANCE

Figure 10 shows how average angle error changes with pedestrian-vehicle distance when using 2, 4 and 6 antennas in J-CSI. The angle estimation error increases with the distance, regardless of the number of antennas. This is because the signal strength decreases as the distance increases, which leads to a reduced SNR and an increased error in angle estimation.

Considering this result, the positioning precision will be improved by assigning different weights to vehicles, with a

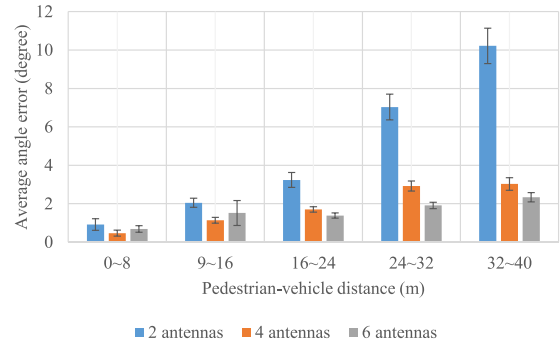


FIGURE 10. Average angle error and 95% confidence interval for each range of pedestrian-vehicle distances.

larger weight for a vehicle with a shorter pedestrian-vehicle distance. This can be achieved by adjusting the measurement noise R in (20).

5) INFLUENCE OF THE NUMBER OF CSI FROM MULTIPLE TIMINGS

The number of CSI acquisitions for multiple timings in J-CSI is changed from 2, 4 to 6, and the average angle estimation error is shown in Figure 11. For any number of antennas, the larger the number of CSI acquisitions for multiple timings, the higher the precision, but the difference is larger when the number of antennas is small. This is because the spatial resolution of the angle, computed from the CSI in the spatial axis alone, is insufficient when the number of antennas is small. Using the CSI in the temporal axis helps to improve the performance. But this improvement gradually diminishes when the number of antennas increases. This is because with more antennas, the CSI in the spatial axis alone is enough to obtain high resolution, even without the CSI in the temporal axis.

6) INFLUENCE OF THE INTERFERENCE WAVE

The influence of the interference wave in J-CSI is investigated. It should be noticed that a signal from a vehicle is leveraged only when it is correctly received, i.e., when the SIR (Signal to Interference Ratio) is high enough. In addition, with the carrier sense mechanism in vehicular communications, the interference does not always occur.

Figure 12 shows how the average angle error changes with SIR in J-CSI, assuming that an interference wave always exists. When the number of antennas is large, the influence of interference waves is very small. This is because the interference wave and the target signal are successfully separated by the MUSIC method. In the MUSIC method, the AoA of multiple arrival signals can be estimated separately from the MUSIC spectrum. Therefore, even though an interference occurs in the received signal, it does not affect the angle estimation of the target LoS wave, if it comes from a different direction.

When the number of antennas is small, the angle resolution is relatively low. The interference waves cannot be separated sufficiently from the LoS wave, and an obvious error occurs in angle estimation. This error increases as SIR gets smaller,

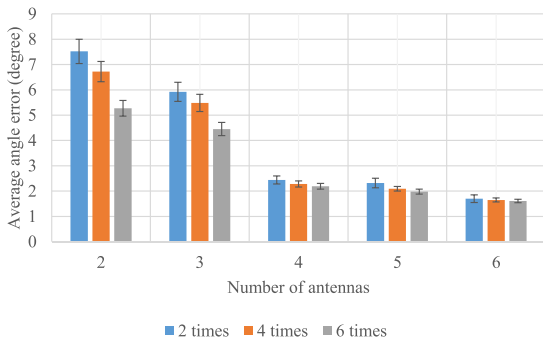


FIGURE 11. Average angle error and 95% confidence interval for each number of CSI acquired from multiple timings in a same packet.

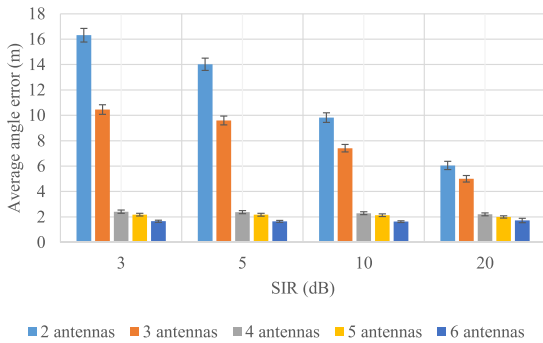


FIGURE 12. Average angle error and 95% confidence interval for each SIR.

but the impact of SIR is not so large. Considering that the increase in angle error is small even with a small number of antennas and that interference waves do not occur every time, the influence of the interference wave on the angle estimation is considered to be quite small.

C. RESULTS FOR PEDESTRIAN POSITIONING

1) COMPARISON WITH OTHER METHODS

Figure 13 shows how the average horizontal positioning error changes with the number of antennas in J-CSI, S-CSI, T-CSI, ESPRIT and Root-WSF. The results for each method are not shown when the number of antennas is not applicable. When positioning is performed using GPS alone, the average horizontal positioning error is 18.87m. By using vehicular signals together, the positioning error is significantly reduced in all methods. When the number of antennas is 2, J-CSI reduces the positioning error by 59% compared with S-CSI, by 17% compared with T-CSI (with a single antenna). When the number of antennas increases to 6, the error reductions by J-CSI, compared with S-CSI and T-CSI, are 8% and 58%, respectively. Because other conditions, except the angle estimation function, are the same in all methods, it is reasonable to attribute the improvement of positioning precision to the refined angle estimation in J-CSI.

2) INFLUENCE OF TRANSMISSION FREQUENCY

The transmission frequency of the vehicular signal is changed from 700MHz to 2.4GHz and 5.9GHz, and the horizontal positioning error in J-CSI is investigated. The results are

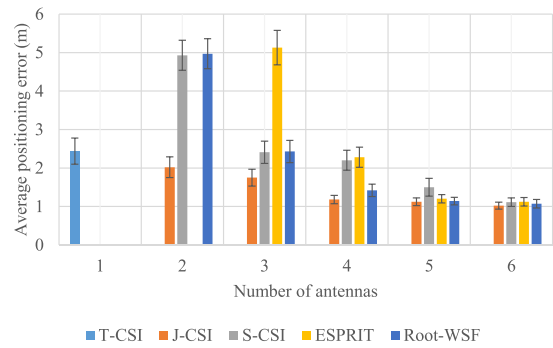


FIGURE 13. Average horizontal positioning error and 95% confidence interval for each method.

shown in Figure 14. Similar to the result in Sec.IV.B.3), the positioning error is lower in 5.9GHz than in 2.4GHz, but is relatively low in 700MHz, when compared with the angle estimation error. This is because the decrease in frequencies leads to a smaller attenuation of the signal strength at the same distance, which improves the precision of distance estimation. Therefore, the angle error in 700MHz is compensated by precise distance information and it leads to a small positioning error.

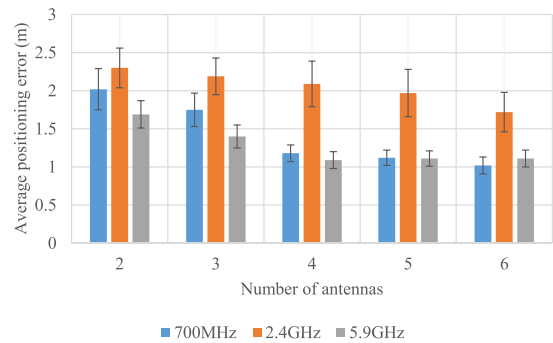


FIGURE 14. Average horizontal positioning error and 95% confidence interval for each frequency band.

3) INFLUENCE OF THE NUMBER OF VEHICLES

In the simulations so far, all the vehicles available for positioning are used. Here, the number of vehicles used in each scene is changed in order to investigate its impact on the positioning precision. Figure 15 shows how the average horizontal positioning error changes with the number of vehicles in J-CSI. Regardless of the number of antennas, the positioning precision improves with the number of vehicles. This is because the distance/angle estimation errors are smoothed as the number of vehicles increases. This is similar to GPS positioning where the positioning precision improves with the number of satellites [34]. However, the positioning error approaches a steady value (error bound) when there are 6 vehicles or more. It indicates that the impact of distance/angle estimation errors cannot be completely removed by smoothing. This error bound can be further reduced by improving the distance/angle estimation precision.

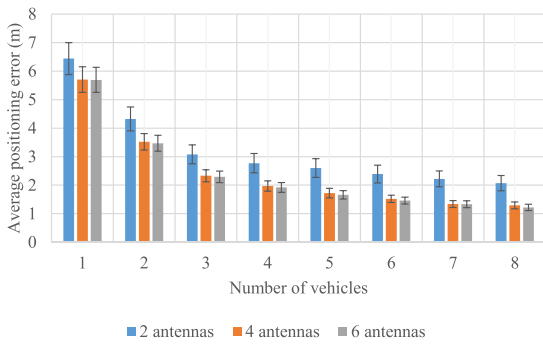


FIGURE 15. Average horizontal positioning error and 95% confidence interval for each number of vehicles.

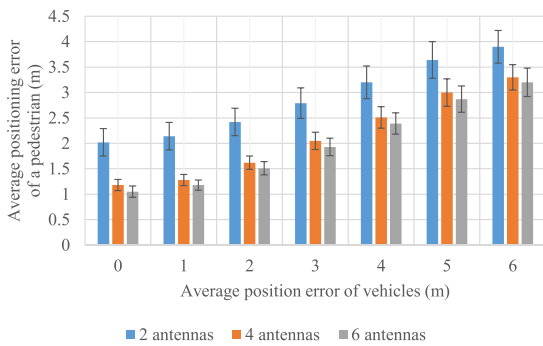


FIGURE 16. Average horizontal positioning error of a pedestrian and 95% confidence interval for each average position error of vehicles.

4) INFLUENCE OF THE POSITION ERROR OF VEHICLES

In the simulations so far, the position of each vehicle is assumed to be accurate without errors. But in a real system, vehicles also have position errors, although smaller compared with that of pedestrians. Here, the vehicular position error is assumed to follow a standard distribution based on the average error of each vehicle used for pedestrian positioning, and its influence is investigated.

Figure 16 shows how the average horizontal position error of a pedestrian in J-CSI changes with vehicle position errors. Generally, the positioning error of a pedestrian increases with the vehicle position error, and has a similar trend for different numbers of antennas. But the pedestrian positioning error is not as large as the vehicle position error. This is because the influence of the vehicle position error is smoothed and reduced by using multiple vehicles (the average number of vehicles is 10) at the same time and by using a Kalman filter.

V. CONCLUSION

Based on our previous methods that exploit V2V communication signals together with GPS signals for pedestrian positioning by estimating pedestrian-vehicle distances/angles, in this paper, we have proposed to further improve the precision of estimating pedestrian-vehicle angles by combining the spatial and temporal changes of CSI. In this method, CSI is acquired from multiple antennas at multiple receiving timings in a single packet, and the phase changes in the spatial axis and the temporal axis are jointly leveraged to estimate

the pedestrian-vehicle angle, by using the modified MUSIC method. On this basis, the pedestrian positioning performance is also evaluated, by considering different factors such as the number of antennas, the frequency band, the number of vehicles as anchors, and vehicle position errors.

Extensive 3D ray tracing simulations confirm that the pedestrian-vehicle angle information plays an important role in pedestrian positioning, and its estimation, relying merely on spatial or temporal changes of CSI, leads to a limited performance. In comparison, combining spatial/temporal changes of CSI can effectively improve the performance of both angle estimation and positioning precision. The performance relies more on temporal CSI when the number of antennas is small and depends more on spatial CSI as the number of antennas increases. With two antennas available on most smartphones and tablets, the performance is significantly improved compared to the base method that uses only spatial changes of CSI. A similar effect can be achieved by the base method that uses only temporal changes of CSI, but by using spatial changes of CSI together, the performance can be further improved when the number of antennas increases. This is important considering that the number of antennas mounted on mobile devices is expected to increase (Some smartphones and tablets already have four antennas mounted). In the future we will further improve and evaluate the proposed method in different environments.

Positioning via wireless signals heavily depends on two key factors, distance measurement and angle estimation. With the widespread of massive MIMO techniques in 5G, it is expected that higher precision of AoA estimation will be achieved at the base station, and AoA estimation will be extended from 2D to 3D to facilitate 3D positioning of flying objects such as drones. Instead of measuring the distance via CSI information, fine time measurement, as a new feature in IEEE 802.11bd, aims to directly measure the flying time from the round-trip delay. But it faces the problem of real-time measurement. An aggressive solution to this problem is to compare the phase difference between multiple frequencies in wireless signals, so as to compute the flying time in one transmission. But how to solve phase ambiguity will be a challenge. In the future, we will investigate how to use new technologies to further improve pedestrian positioning precision.

REFERENCES

- [1] "Inter-vehicle communication message specifications," ITS Connect Promotion Consortium, Tokyo, Japan, Tech. Rep. ITS Connect TD-001 Ver.1.0, 2015.
- [2] UTMS Society of Japan. *DSSS [Driving Safety Support Systems]*. Accessed: Mar. 17, 2021. [Online]. Available: <http://www.utms.or.jp/english/system/dsss.html>
- [3] *Toyota, ITS Connect*. Accessed: Mar. 17, 2021. [Online]. Available: <https://toyota.jp/technology/safety/itsconnect/>
- [4] S. Tang, K. Saito, and S. Obana, "Transmission control for reliable pedestrian-to-vehicle communication by using context of pedestrians," in *Proc. IEEE Int. Conf. Veh. Electron. Saf. (ICVES)*, Nov. 2015, pp. 41–47.
- [5] Y. Patou, S. Obana, and S. Tang, "Improvement of pedestrian positioning precision by using spatial correlation of multipath error," in *Proc. IEEE Int. Conf. Veh. Electron. Saf. (ICVES)*, Sep. 2018, pp. 1–8.

- [6] L.-T. Hsu, F. Chen, and S. Kamijo, "Evaluation of multi-GNSSs and GPS with 3D map methods for pedestrian positioning in an urban canyon environment," *IEICE Trans. Fundam. Electron., Commun. Comput. Sci.*, vol. E98.A, no. 1, pp. 284–293, 2015.
- [7] C. Kwon and I. Hwang, "Constrained stochastic hybrid system modeling to road map–GPS integration for vehicle positioning," in *Proc. IEEE 55th Conf. Decis. Control (CDC)*, Dec. 2016, pp. 314–319.
- [8] L. Youwen, "Forecast map matching model for vehicle-borne navigation based on roadway characteristic," in *Proc. Int. Conf. Optoelectron. Image Process. (ICOIP)*, vol. 1, 2010, pp. 569–571.
- [9] R. Yamashita, S. Tang, and S. Obana, "Proposal and evaluation of pedestrian positioning method by using signals from both GPS satellites and vehicles," *IPSS J.*, vol. 59, no. 1, pp. 113–123, 2018.
- [10] S. Tang and S. Obana, "Improving performance of pedestrian positioning by using vehicular communication signals," *IET Intell. Transp. Syst.*, vol. 12, no. 5, pp. 366–374, Jun. 2018.
- [11] K. Toda, S. Tang, and S. Obana, "High-precision pedestrian positioning by using radio signals from vehicles and roadside units," in *Proc. Int. Conf. Electron., Inf., Commun. (ICEIC)*, Jan. 2019, pp. 1–8.
- [12] W. Komamiya, S. Tang, and S. Obana, "Radiation angle estimation and high-precision pedestrian positioning by tracking change of channel state information," *Sensors*, vol. 20, no. 5, p. 1430, Mar. 2020.
- [13] Z. Yang, J. Li, P. Stoica, and L. Xie, "Sparse methods for direction-of-arrival estimation," in *Academic Press Library in Signal Processing*, vol. 7, R. Chellappa and S. Theodoridis, Eds. New York, NY, USA: Academic, 2018, pp. 509–581.
- [14] Z. Yang, Z. Zhou, and Y. Liu, "From RSSI to CSI: Indoor localization via channel response," *ACM Comput. Surv.*, vol. 46, no. 2, pp. 1–32, Nov. 2013.
- [15] Y. Xie, Z. Li, and M. Li, "Precise power delay profiling with commodity WiFi," in *Proc. 21st Annu. Int. Conf. Mobile Comput. Netw.*, Sep. 2015, pp. 53–64.
- [16] D. Vasisht, S. Kumar, and D. Katabi, "Decimeter-level localization with a single Wi-Fi access point," in *Proc. NSDI*, 2016, pp. 165–178.
- [17] M. Groth, M. Rzymowski, K. Nyka, and L. Kulas, "ESPAR antenna-based WSN node with DoA estimation capability," *IEEE Access*, vol. 8, pp. 91435–91447, 2020.
- [18] S. Sen, J. Lee, K.-H. Kim, and P. Congdon, "Avoiding multipath to revive inbuilding WiFi localization," in *Proc. 11th Annu. Int. Conf. Mobile Syst., Appl., Services (MobiSys)*, 2013, pp. 249–262.
- [19] S. Wielandt and L. Strycker, "Indoor multipath assisted angle of arrival localization," *Sensors*, vol. 17, no. 11, p. 2522, Nov. 2017.
- [20] R. O. Schmidt, "Multiple emitter location and signal parameter estimation," *IEEE Trans. Antennas Propag.*, vol. AP-34, no. 3, pp. 276–280, Mar. 1986.
- [21] A. Hu, T. Lv, H. Gao, Z. Zhang, and S. Yang, "An ESPRIT-based approach for 2-D localization of incoherently distributed sources in massive MIMO systems," *IEEE J. Sel. Topics Signal Process.*, vol. 8, no. 5, pp. 996–1011, Oct. 2014, doi: [10.1109/JSTSP.2014.2313409](https://doi.org/10.1109/JSTSP.2014.2313409).
- [22] M. Jansson, A. L. Swindlehurst, and B. Ottersten, "Weighted subspace fitting for general array error models," *IEEE Trans. Signal Process.*, vol. 46, no. 9, pp. 2484–2498, 1998.
- [23] Y.-L. Ban, C. Li, C.-Y.-D. Sim, G. Wu, and K.-L. Wong, "4G/5G multiple antennas for future multi-mode smartphone applications," *IEEE Access*, vol. 4, pp. 2981–2988, 2016, doi: [10.1109/ACCESS.2016.2582786](https://doi.org/10.1109/ACCESS.2016.2582786).
- [24] T.-J. Shan, M. Wax, and T. Kailath, "On spatial smoothing for direction-of-arrival estimation of coherent signals," *IEEE Trans. Acoust., Speech, Signal Process.*, vol. ASSP-33, no. 4, pp. 806–811, Aug. 1985.
- [25] R. T. Williams, S. Prasad, A. K. Mahalanabis, and L. H. Sibul, "An improved spatial smoothing technique for bearing estimation in a multipath environment," *IEEE Trans. Acoust., Speech, Signal Process.*, vol. ASSP-36, no. 4, pp. 425–432, Apr. 1988.
- [26] R. Zhang, Y.-H. Quan, S.-Q. Zhu, L. Yang, Y.-C. Li, and M.-D. Xing, "Joint high-resolution range and DOA estimation via MUSIC method based on virtual two-dimensional spatial smoothing for OFDM radar," *Int. J. Antennas Propag.*, vol. 2018, pp. 1–9, Nov. 2018.
- [27] S. Qin, Y. D. Zhang, and M. G. Amin, "Generalized coprime array configurations for direction-of-arrival estimation," *IEEE Trans. Signal Process.*, vol. 63, no. 6, pp. 1377–1390, Mar. 2015, doi: [10.1109/TSP.2015.2393838](https://doi.org/10.1109/TSP.2015.2393838).
- [28] C. Zhou, Y. Gu, X. Fan, Z. Shi, G. Mao, and Y. D. Zhang, "Direction-of-arrival estimation for coprime array via virtual array interpolation," *IEEE Trans. Signal Process.*, vol. 66, no. 22, pp. 5956–5971, Nov. 2018, doi: [10.1109/TSP.2018.2872012](https://doi.org/10.1109/TSP.2018.2872012).
- [29] Z.-M. Liu, C. Zhang, and P. S. Yu, "Direction-of-arrival estimation based on deep neural networks with robustness to array imperfections," *IEEE Trans. Antennas Propag.*, vol. 66, no. 12, pp. 7315–7327, Dec. 2018, doi: [10.1109/TAP.2018.2874430](https://doi.org/10.1109/TAP.2018.2874430).
- [30] H. Huang, J. Yang, H. Huang, Y. Song, and G. Gui, "Deep learning for super-resolution channel estimation and DOA estimation based massive MIMO system," *IEEE Trans. Veh. Technol.*, vol. 67, no. 9, pp. 8549–8560, Sep. 2018, doi: [10.1109/TVT.2018.2851783](https://doi.org/10.1109/TVT.2018.2851783).
- [31] H. Jiang, Z. Zhang, C.-X. Wang, J. Zhang, J. Dang, L. Wu, and H. Zhang, "A novel 3D UAV channel model for A2G communication environments using AoD and AoA estimation algorithms," *IEEE Trans. Commun.*, vol. 68, no. 11, pp. 7232–7246, Nov. 2020, doi: [10.1109/TCOMM.2020.3011716](https://doi.org/10.1109/TCOMM.2020.3011716).
- [32] B. Yang, P. Zhang, H. Wang, and W. Hong, "Efficient delay and AoA estimation using vector antenna for radio propagation measurements," in *Proc. IEEE Int. Symp. Antennas Propag. USNC-URSI Radio Sci. Meeting*, Jul. 2019, pp. 2125–2126, doi: [10.1109/APUSNCURSINRSM.2019.8888694](https://doi.org/10.1109/APUSNCURSINRSM.2019.8888694).
- [33] H. V. Jemderon, F. Pukelsheim, and S. R. Searle, "On the history of the kronecker product," *Linear Multilinear Algebra*, vol. 14, no. 2, pp. 113–120, 1983.
- [34] C. Specht, M. Mania, M. Skóra, and M. Specht, "Accuracy of the GPS positioning system in the context of increasing the number of satellites in the constellation," *Polish Maritime Res.*, vol. 22, no. 2, pp. 9–14, 2015.



WATARU KOMAMIYA received the B.S. degree in informatics and computer engineering from The University of Electro-Communications, Japan, in 2018, where he is currently pursuing the master's degree with the Graduate School of Informatics and Engineering.



SUHUA TANG (Member, IEEE) received the B.S. degree in electronic engineering and the Ph.D. degree in information and communication engineering from the University of Science and Technology of China, in 1998 and 2003, respectively. From October 2003 to March 2014, he was with the Adaptive Communications Research Laboratories, Advanced Telecommunications Research Institute International (ATR), Japan. Since April 2014, he has been with the Graduate School of Informatics and Engineering, The University of Electro-Communications, Japan. His research interests include green communications, ad hoc and sensor networks, inter-vehicle communications, and high precision positioning. He is currently a member of IEICE and IPSJ.



SADAO OBANA received the B.E., M.E., and Ph.D. degrees from Keio University, Tokyo, Japan, in 1976, 1978, and 1993, respectively. After joining KDDI (former KDD), in 1978, he was engaged in research and development in the field of packet exchange systems, network architecture, OSI (Open Systems Interconnection) protocols, database, distributed processing, network management, and ITS (Intelligent Transport Systems). In 2004, he joined the Advanced Telecommunications Research Institute International (ATR) and was the Director of the Adaptive Communications Research Laboratories, ATR. From 2011 to 2018, he was a Professor with the Graduate School of Informatics and Engineering, The University of Electro-Communications, Japan. He is currently the Executive Director of The University of Electro-Communications. He received the Award of Minister of Education, Culture, Sports, Science and Technology in 2001. He is also a member of the Institute of Electronics, Information and Communication Engineers (IEICE) and a Fellow of the Information Processing Society of Japan (IPSSJ).